Ground and Low-Lying States of the Vanadium Boride Cation, VB^+: An ab Initio Investigation

Apostolos Kalemos and Aristides Mavridis*

Department of Chemistry, Laboratory of Physical Chemistry, National and Kapodistrian University of Athens, P.O. Box 64004, 157 10 Zografou, Athens, Greece

Received: December 4, 1998

We have examined the vanadium boride system, VB^+, by ab initio MRCI (CASSCF + 1 + 2) methods. In addition to the ground $X^6\Sigma^+$ state, 33 low-lying states have been studied spanning an energy range of less than 2.5 eV. With the exception of four states, all other states are bound with respect to the ground-state products. We report full potential energy curves, total energies, dissociation energies, bond lengths, and harmonic frequencies. Furthermore, we discuss extensively the bonding mechanisms of different states by the aid of valence bond pictures.

1. Introduction

Continuing our work on diatomic borides with first-row transition metal cations,[1] we report detailed electronic structure calculations on the vanadium boride molecule, VB^+. The goal of this study is the determination of accurate dissociation energies and binding modes of the ground and a series of low-lying states. In essence, all states examined stem from the ground ^2P state of the B atom, and the ground $a^5D(3d^4)$ and the second excited $a^3F(4s^13d^3)$ state of the V^+ ion. All quartets and sextets tracing their origin to the V^+ a^5D ground state have been examined, namely, 18 states of $^{4,6}\Sigma^+(2)$, $^{4,6}\Sigma^-$, $^{4,6}\Pi(3)$, $^{4,6}\Delta(2)$, and $^{4,6}\Phi$ symmetry. For purely technical reasons, no states emanating from the first excited a^5F state of the V^+ cation have been examined. For the same reasons, only half of the 24 states resulting from the second a^3F state of V^+ have been completed, i.e., $^2\Sigma^+$, $^2\Sigma^-(2)$, $^2\Pi(3)$, $^2\Delta(3)$, $^2\Phi(2)$, and $^2\Gamma$. Four more states of $^2\Sigma^+(2)$, $^2\Delta$, and $^2\Gamma$ symmetry which correlate to higher states of the V^+ cation have also been (partially) examined. All in all, 34 states were calculated spanning an energy range of 2.5 eV, 30 of which are bound with respect to their ground-state fragments. For 30 states, full potential energy curves (PEC) were constructed at the multireference configuration interaction level; we report total energies, dissociation energies, equilibrium bond distances, harmonic frequencies, and energy gaps.

The structure of the article is in line with our previous reports;[1] after a short discussion on technical details, we touch upon the atomic states, and a long section follows on results and discussion. We close with a synopsis on the salient features of our findings.

2. Basis Sets and Methodology

For the V atom, the ANO basis set 20s15p10d6f4g of Bauschlicher[2] was used but with the 4g functions removed, generalized contracted to 7s6p4d3f. For the B atom, the triple-ζ correlation consistent basis (cc-pVTZ) 10s5p2d1f of Dunning[3] was employed, contracted to 4s3p2d1f. The resulting one-electron space contains 96 spherical Gaussian functions. The ground VB^+ state ($X^6\Sigma^+$) was also computed with a cc-pVQZ on boron, but the overall differences from the triple-ζ basis were insignificant (vide infra).

Considering the V^+ $1s^22s^22p^63s^23p^6$ and the $1s^2$ electrons of B as "core", we are dealing with a seven "valence" (active) electron problem. This system generates $^{2S+1}|\Lambda|$ states with spin multiplicities of 2, 4, 6, and 8. Disregarding the octet states (which correlate to the ^4P state of the B atom), all other multiplicities have been considered. With the exception of the sextet states which can be formally described by a single reference wave function, the quartets and doublets demand a multireference description. In the present work, a CASSCF (complete active space SCF) + single + double replacements (=MRCI) methodology is used, essentially the only method available[4] that is variational and, due to the relative small number of active electrons, practically size consistent and size extensive.[5,6]

Our reference CAS space is comprised of 10 orbital functions, namely, 4s + 3d on V^+ and 2s + 2p on B. Depending on the symmetry, the CASSCF wave function contains 500 (sextets) to 3500 (doublets) configuration functions (CFs). Although all calculations were performed under C_{2v} symmetry restrictions, our CASSCF wave functions display axial angular momentum symmetry, viz., $|\Lambda| = 0$, 1, 2, 3, and 4 or $\Sigma^{\pm}$, Π, Δ, Φ, and Γ, respectively.

Valence correlation energy was extracted by single and double excitations out of the reference CAS space (MRCI). To keep the computations manageable, the "internal contraction" technique (icMRCI)[7] was used. Thus, our largest MRCI expansion of about 6 300 000 CFs is contracted to ~600 000 CFs.

Due to the intricate nature of the PECs, we were forced to use the state-average (SA) technique.[8,9] Numerical experiments for the ground $X^6\Sigma^+$ state of the VB^+, performed with and without the SA method, showed total energy losses of less than 2 mhartrees, in agreement with our previous experience.[1] It was also found that the SA method is responsible for size extensivity errors of about 1.5 mhartrees, while extensivity errors without the SA approach are not larger than 0.1 mhartree. However, dissociation energies (D_e) are negligibly affected by the SA approach due to practical cancellation of size nonextensivity and total energy losses. Finally, no basis set superposition effects were taken into account in the calculation of D_e's, judging as adequate enough our basis sets size.

10.1021/jp984614q CCC: $18.00
Published on Web 04/09/1999

TABLE 1: Total Energies (hartree) of the V(a^4F, a^6D), V^+(a^5D, a^5F, a^3F), B(^2P, ^4P) Terms and Corresponding Energy Splittings (eV) in Different Methodologies

	V	
method	a^4F	a^6D
NHF[a]	−942.884338	−942.879783
SCF	−942.886073	−942.881204
CISD	−942.959237	−942.949814
sa-SCF[b]	−942.883964	−942.879356
CISD	−942.957440	−942.948456

	V^+		
method	a^5D	a^5F	a^3F
NHF[c]	−942.670784		
SCF	−942.670609	−942.677988	−942.644568
CISD	−942.722825	−942.711400	−942.685022
sa-SCF[b]	−942.670316	−942.675861	−942.642509
CISD	−942.722784	−942.709840	−942.683583

	B	
method	^2P	^4P
NHF[a]	−24.529061	
SCF	−24.528147	−24.451286
CISD	−24.596634	−24.467237
sa-SCF[b]	−24.528098	−24.449313
CISD	−24.596552	−24.467211
sa-CASSCF[b]	−24.559329	-
MRCI	−24.598396	-

	energy splittings			
	V	V^+		B
method	$^6D \leftarrow {}^4F$	$^5F \leftarrow {}^5D$	$^3F \leftarrow {}^5F$	$^4P \leftarrow {}^2P$
sa-SCF[b]	0.125	0.151	0.908	2.144
CISD	0.246	0.363	0.700	3.520
MRCI[d]				3.570
expt[e]	0.245	0.337	0.741	3.571

[a] Numerical Hartree−Fock, ref 11. [b] Spherically averaged SCF or CASSCF. [c] Numerical Hartree−Fock, ref 12. [d] Difference between ^4P(CISD) and ^2P(MRCI). [e] Reference 13.

All calculations were done with the MOLPRO suite of codes.[10]

3. The Atoms

Table 1 reports total energies of the V^+ $a^5D(3d^4)$, $a^5F(4s^1$-$3d^3)$, and $a^3F(4s^13d^3)$ and of the B $^2P(2s^22p^1)$ and $^4P(2s^12p^2)$ spectroscopic terms in different methodologies, as well as corresponding energy splittings. For completeness, total energies of the $a^4F(4s^23d^3)$ and $a^6D(4s^13d^4)$ terms and the $^6D \leftarrow {}^4F$ splitting of V are also given. Small energy differences between SCF and spherically averaged (sa) SCF are due to the contaminated angular momentum (spatial polarization) SCF vectors.[14] All energy gaps are in very good agreement with experimental findings, with the largest absolute discrepancy being 0.95 kcal/mol, (V^+($^3F \leftarrow {}^5F$)).

4. Results and Discussion

Tables 2−4 present total energies (E), bond lengths (R_e), dissociation energies (D_e), harmonic frequencies (ω_e), and energy gaps (T_e) of all states studied: 9 sextets, 9 quartets, and 16 doublets of $\Sigma^{\pm}$, Π, Δ, Φ, and Γ (spatial) symmetry. The results reported are at the CASSCF, icMRCI, and icMRCI+Q (icMRCI + multireference Davidson correction[15]) level. An overall picture of the entangled PECs is shown in Figure 1, while Figure 2 presents a level state diagram; numbers in front of the state symbols refer to absolute energy ordering with respect to the ground (X) state.

In the ensuing discussion, the sextets are presented first, followed by the quartets, and finally by the doublets.

TABLE 2: Energies E (hartree), Bond Distances R_e (Å), Dissociation Energies D_e (kcal/mol), Harmonic Frequencies ω_e (cm^{-1}), and Energy Gaps T_e (kcal/mol) of the $X^6\Sigma^+$, $1^6\Delta$, $5^6\Pi$, $18^6\Phi$, $19^6\Sigma^+$, $22^6\Pi$, $27^6\Delta$, $28^6\Pi$, and $29^6\Sigma^-$ States of VB^+ in Ascending Energy Order

state	method[a,b]	−E	R_e	D_e	ω_e	T_e[c]
$X^6\Sigma^+$	CASSCF					
	icMRCI	967.387 70	2.061	42.7	496	0.0
	icMRCI+Q	967.3953	2.068	45.5	496	
$1^6\Delta$	CASSCF					
	icMRCI	967.382 91	2.163	39.9	543	3.0
	icMRCI+Q	967.3890	2.172	41.7	523	
$5^6\Pi$	CASSCF	967.261 58	2.736	15.3	196	
	icMRCI	967.361 61	2.339	26.6	366	16.4
	icMRCI+Q	967.3687	2.337	28.9	374	
$18^6\Phi$	CASSCF	967.235 23	2.5	1.4		
	icMRCI	967.343 10	2.190	14.9	416	28.0
	icMRCI+Q	967.3514	2.189	17.7	502	
$19^6\Sigma^+$	CASSCF	967.241 16	2.435	5.6	237	
	icMRCI	967.342 60	2.275	14.6		28.3
	icMRCI+Q	967.3490	2.228	16.1	418	
$22^6\Pi$	CASSCF	967.235 70	2.912	1.7		
	icMRCI	967.340 16	2.173	13.0	564	29.8
	icMRCI+Q	967.3483	2.180	15.7	607	
$27^6\Delta$	CASSCF					
	icMRCI	967.325 73	2.450	4.0	164	38.9
	icMRCI+Q					
$28^6\Pi$	CASSCF	967.234 55	2.964	1.1	102	
	icMRCI	967.325 18	2.642	3.8	161	39.2
	icMRCI+Q	967.3300	2.561	4.3	159	
$29^6\Sigma^-$	CASSCF					
	icMRCI	967.324 46	2.440	3.2		39.7
	icMRCI+Q					

[a] The CASSCF results have been obtained by the state-average method. [b] +Q refers to the multireference Davidson correction, ref 15. [c] 1 hartree = 627.51 kcal/mol.

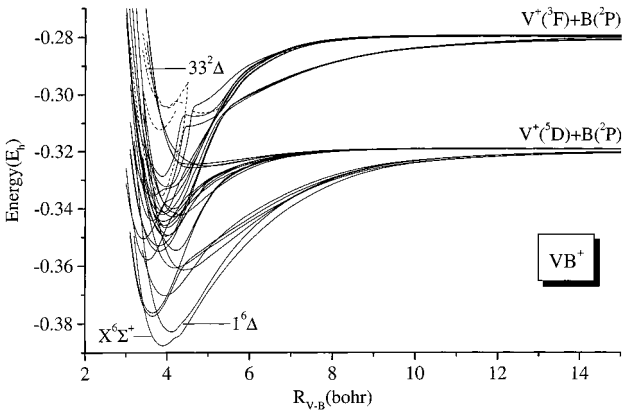

Figure 1. MRCI potential energy curves of all 34 VB^+ states studied, dashed lines present partially computed PECs.

4.1. Sextets. Table 2 presents our numerical findings, and Figure 3 shows PECs of all sextet states.

Ground $X^6\Sigma^+$ State. At equilibrium, the HF configuration,

$$X|^6\Sigma^+\rangle \approx |1\sigma^2(2s_B^2)2\sigma^1 1\delta_+^1 1\pi_x^1 1\pi_y^1 1\delta_-^1\rangle$$

prevails (C_o = 0.87), while the asymptotic fragments are described by the product $X|^6\Sigma^+\rangle = |^5D; M = 0\rangle \otimes |^2P; M = 0\rangle$. The binding interaction is represented faithfully by the valence-

TABLE 3: Energies E (hartree), Bond Distances R_e (Å), Dissociation Energies D_e (kcal/mol), Harmonic Frequencies ω_e (cm^{-1}), and Energy Gaps T_e (kcal/mol) of the $2^4\Pi$, $3^4\Phi$, $4^4\Delta$, $6^4\Sigma^+$, $8^4\Pi$, $12^4\Delta$, $13^4\Sigma^-$, $15^4\Pi$, and $16^4\Sigma^+$ States of VB^+ in Ascending Energy Order

state	method[a,b]	$-E$	R_e	D_e	ω_e	T_e
$2^4\Pi$	CASSCF	967.273 91	1.915	23.0	631	
	icMRCI	967.377 54	1.926	36.6	595	6.4
	icMRCI+Q	967.3831	1.931	37.9	586	
$3^4\Phi$	CASSCF	967.274 33	1.922	25.9	642	
	icMRCI	967.376 41	1.928	35.8	599	7.1
	icMRCI+Q	967.3818	1.932	36.7	589	
$4^4\Delta$	CASSCF	967.267 65	2.056	17.9	482	
	icMRCI	967.370 35	2.092	32.0	455	10.9
	icMRCI+Q	967.3762	2.104	33.6	444	
$6^4\Sigma^+$	CASSCF	967.262 66	2.744	14.6	217	
	icMRCI	967.360 78	2.215	25.8	398	16.9
	icMRCI+Q	967.3673	2.211	29.9	424	
$8^4\Pi$	CASSCF	967.251 79	2.283	11.8	547	
	icMRCI	967.356 00	2.241	23.0	582	19.9
	icMRCI+Q	967.3600	2.229	23.0	578	
$12^4\Delta$	CASSCF	967.242 87	2.120	6.7	451	
	icMRCI	967.349 76	2.100	19.1	523	23.8
	icMRCI+Q	967.3565	2.103	20.8	527	
$13^4\Sigma^-$	CASSCF	967.241 64	2.138	5.9	518	
	icMRCI	967.349 48	2.128	18.9	562	24.0
	icMRCI+Q	967.3568	2.134	20.9	555	
$15^4\Pi$	CASSCF					
	icMRCI	967.346 07	2.092	16.9	650	26.1
	icMRCI+Q	967.3534	2.095	19.0	662	
$16^4\Sigma^+$	CASSCF	967.237 76	2.078	3.5	402	
	icMRCI	967.344 55	2.068	15.8	491	27.1
	icMRCI+Q	967.3512	2.072	17.5	495	

[a] The CASSCF results have been obtained by the state-average method. [b] +Q refers to the multireference Davidson correction, ref 15.

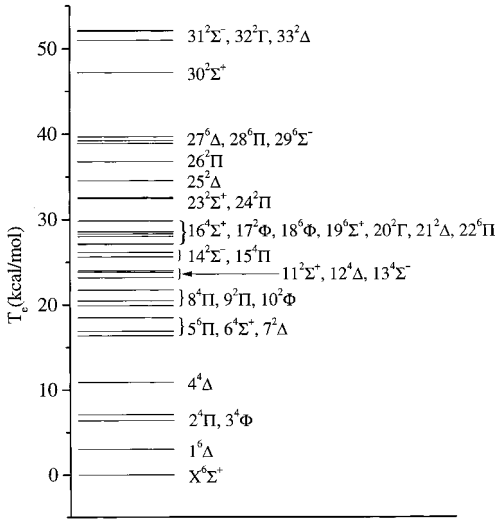

Figure 2. Relative energy level diagram of the VB^+ system.

bond-Lewis (vbL) icon

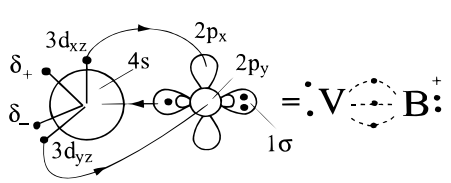

suggesting two half π bonds stemming from the V^+ ion, and a half σ bond stemming from the B atom. The CAS equilibrium atomic populations are (first entry V, second entry B)

$$4s^{0.21}4p_z^{0.09}3d_{z^2}^{0.52}3d_{xz}^{0.61}3d_{yz}^{0.61}3d_{x^2-y^2}^{1.0}3d_{xy}^{1.0}/2s^{1.60}2p_z^{0.59}2p_x^{0.38}2p_y^{0.38}$$

TABLE 4: Energies E (hartree), Bond Distances R_e (Å), Dissociation Energies D_e (kcal/mol), Harmonic Frequencies ω_e (cm^{-1}), and Energy Gaps T_e (kcal/mol) of the $7^2\Delta$, $9^2\Pi$, $10^2\Phi$, $11^2\Sigma^+$, $14^2\Sigma^-$, $17^2\Phi$, $20^2\Gamma$, $21^2\Delta$, $23^2\Sigma^+$, $24^2\Pi$, $25^2\Delta$, $26^2\Pi$, $30^2\Sigma^+$, $31^2\Sigma^-$, $32^2\Gamma$, and $33^2\Delta$ States of VB^+ in Ascending Energy Order

state	method[a,b]	$-E$	R_e	D_e[c]	ω_e	T_e
$7^2\Delta$	CASSCF	967.251 30	1.863	30.9	659	
	icMRCI	967.358 23	1.858	49.2	739	18.5
	icMRCI+Q	967.3650	1.862	50.9	728	
$9^2\Pi$	CASSCF	967.252 97	2.033	31.8	498	
	icMRCI	967.355 09	2.009	47.2	541	20.5
	icMRCI+Q	967.3610	2.014	48.4	523	
$10^2\Phi$	CASSCF	967.251 92	2.036	31.2	486	
	icMRCI	967.353 06	2.006	46.0	509	21.7
	icMRCI+Q	967.3589	2.017	47.2	492	
$11^2\Sigma^+$	CASSCF	967.247 11	1.800	28.4	689	
	icMRCI	967.350 77	1.804	44.6	685	23.2
	icMRCI+Q	967.3560	1.809	45.4	675	
$14^2\Sigma^-$	CASSCF	967.243 92	2.120	26.2	493	
	icMRCI	967.346 88	2.104	41.5	522	25.6
	icMRCI+Q	967.3533	2.108	42.9	534	
$17^2\Phi$	CASSCF	967.240 22	1.918	24.1	731	
	icMRCI	967.344 42	1.924	40.4	719	27.2
	icMRCI+Q	967.3504	1.927	41.6	713	
$20^2\Gamma$	CASSCF	967.240 66	2.056	24.2	506	
	icMRCI	967.342 20	2.051	39.1	521	28.6
	icMRCI+Q	967.3482	2.060	40.4	502	
$21^2\Delta$	CASSCF	967.238 01	2.065	22.7	779	
	icMRCI	967.342 14	2.053	39.2	692	28.6
	icMRCI+Q	967.3486	2.060	40.8	667	
$23^2\Sigma^+$	CASSCF	967.232 63	2.064			
	icMRCI	967.335 94	2.064			32.5
	icMRCI+Q	967.3422	2.064			
$24^2\Pi$	CASSCF	967.231 77	1.911	18.8	585	
	icMRCI	967.335 77	1.921	35.0	572	32.6
	icMRCI+Q	967.3417	1.929	36.2	562	
$25^2\Delta$	CASSCF	967.228 04	2.108	16.6	603	
	icMRCI	967.332 66	2.096	32.8	580	34.5
	icMRCI+Q	967.3399	2.101	34.7	591	
$26^2\Pi$	CASSCF	967.223 98	2.059	14.2	805	
	icMRCI	967.329 11	2.055	31.1	750	36.8
	icMRCI+Q	967.3362	2.057	33.0	769	
$30^2\Sigma^+$	CASSCF	967.204 23	2.033		566	
	icMRCI	967.312 48	2.016		588	47.2
	icMRCI+Q	967.3196	2.016		586	
$31^2\Sigma^-$	CASSCF	967.213 86	2.708	7.5	480	
	icMRCI	967.306 49	2.549	16.8	249	51.0
	icMRCI+Q	967.3137	2.528	18.9	309	
$32^2\Gamma$	CASSCF	967.195 46	2.139		610	
	icMRCI	967.305 06	2.119		581	51.9
	icMRCI+Q	967.3124	2.116		529	
$33^2\Delta$	CASSCF					
	icMRCI	967.304 62	2.12			52.1
	icMRCI+Q					

[a] The CASSCF results have been obtained by the state-average method. [b] +Q refers to the multireference Davidson correction, ref 15. [c] The D_e is calculated with respect to the ^3F state of V^+.

in full support of the above picture. 0.8 e^- are transferred from B to a $(4s4p_z3d_{z^2})^{0.8}$ V^+ hybrid via the σ-frame, while 0.8 e^- are moving from V^+ to B through the π-frame. Notice that the $\delta_\pm$ ($3d_{x^2-y^2}$, $3d_{xy}$) electrons do not participate in the bonding mechanism being completely localized on the metal. This is also clear by contrasting the $X^6\Sigma^+$ state of VB^+ with the $X^4\Sigma^-$ and $X^5\Delta$ states of ScB^+ [1a] and TiB^+,[1b] respectively. For the latter, D_e, R_e, and ω_e values are (44.9, 47.6) kcal/mol, (2.160, 2.102) Å, and (513, 519) cm^{-1}, very similar to the corresponding values of VB^+, Table 2. The decrease in bond distance from ScB^+ to TiB^+ to VB^+ by 0.06 and 0.04 Å follows the regular decrease in the atomic radii of Sc, Ti, and V atoms.

Calculations with a quadruple basis set (cc-pVQZ) on boron lowered the absolute energy by 3.7 mhartrees at the MRCI level

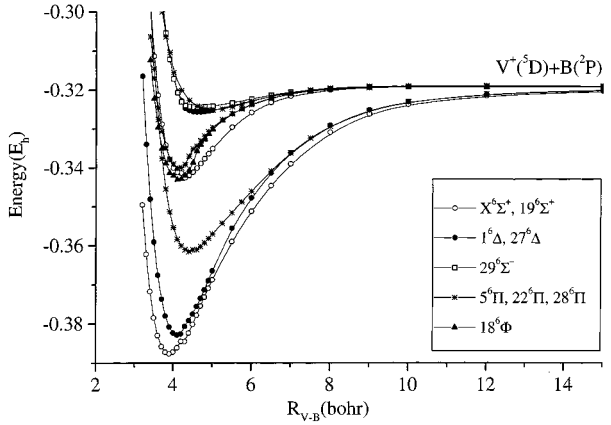

Figure 3. Potential energy curves of nine sextet states of Σ^+ (○), Σ^- (□), Π (∗), Δ (●), and Φ (▲) spatial symmetry.

and decreased the bond length by 0.01 Å, but the D_e remained the same. No further calculations were done with the quadruple basis set.

Figure 3 presents the PECs for all studied sextets. Notice the small irregularity in the $X^6\Sigma^+$ PEC around 4.3 bohr, which is caused by the $19^6\Sigma^+$ state interacting with the $X^6\Sigma^+$ state, located 28.3 kcal/mol above the ground state.

$1^6\Delta$ State (2nd of the Sextets). This state results by moving a δ e^- of the $X^6\Sigma^+$ state to an orbital of σ symmetry:

$$1|^6\Delta\rangle \approx |1\sigma^2 2\sigma^1 3\sigma^1 1\pi_x^1 1\pi_y^1 1\delta^1\rangle$$

($C_o = 0.90$). At infinity, the wave function is described by $1|^6\Delta\rangle = |^5\mathrm{D};\ M = \pm 2\rangle \otimes |^2\mathrm{P};\ M = 0\rangle$. The CAS equilibrium atomic distributions are

$$4s^{0.73}4p_z^{0.08}3d_{z^2}^{0.86}3d_{xz}^{0.76}3d_{yz}^{0.76}3d_{xy}^{1.0}/2s^{1.62}2p_z^{0.65}2p_x^{0.25}2p_y^{0.25}$$

The above populations dictate the following vbL icon:

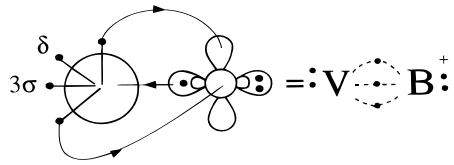

with 0.50 e^- transferred to the B atom through the π frame and 0.73 e^- to the V^+ via the σ frame, resulting to three half bonds and a net charge migration of 0.2 e^- from B to V^+. Compared to the $X^6\Sigma^+$ state an appreciable bond lengthening of 0.10 Å is observed (Table 2), probably due to the presence of two σ electrons.

$5^6\Pi$ State (3rd of the Sextets). The leading configuration ($C_o = 0.95$) and the asymptotic description are given by

$$5|^6\Pi\rangle \approx |1\sigma^2 2\sigma^1 3\sigma^1 1\pi_y^1 1\delta_+^1 1\delta_-^1\rangle$$

and $5|^6\Pi\rangle = |^5\mathrm{D};\ M = \pm 1\rangle \otimes |^2\mathrm{P};\ M = 0\rangle$. The two atoms are held together by a half σ bond and a half π bond, with three spectator electrons of σ and $\delta_\pm$ symmetry. These ideas are pictorially represented by the vbL diagram

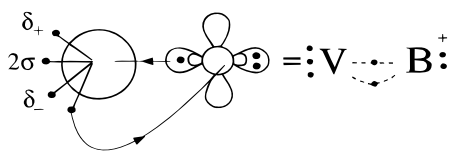

The CAS atomic populations are in complete conformity with the above icon

$$4s^{0.36}4p_z^{0.10}3d_{z^2}^{0.94}3d_{yz}^{0.85}3d_{x^2-y^2}^{1.0}3d_{xy}^{1.0}/2s^{1.74}2p_z^{0.78}2p_x^{0.05}2p_y^{0.20}$$

Approximately 0.15 e^- are moving from V^+ to B via the π system, and 0.46 e^- are transferred from B to the ($4s4p_z$) hybrid of the V^+ cation via the σ frame. Thus, a net charge of 0.2 e^- migrates from B to V^+. As is expected, the bond length in this state increases significantly by 0.28 Å, as compared to the ground $X^6\Sigma^+$ state, with a synchronous drastic decrease in the binding energy; see Table 2.

$18^6\Phi$ State (4th of the Sextets). Asymptotically, this $^6\Phi$ state is represented by the product $18|^6\Phi\rangle = |^5\mathrm{D};\ M = \pm 2\rangle \otimes |^2\mathrm{P};\ M = \pm 1\rangle$ with the following leading distribution

$$18|^6\Phi\rangle \approx 0.66|1\sigma^2 2\sigma^1 1\pi_x^1 1\pi_y^1 (1\delta_+^1 2\pi_y^1 + 2\pi_x^1 1\delta_-^1)\rangle$$

The CAS, close to equilibrium atomic populations, are

$$4s^{0.28}4p_z^{0.09}3d_{z^2}^{0.62}3d_{xz}^{0.96}3d_{yz}^{0.96}3d_{x^2-y^2}^{0.50}3d_{xy}^{0.50}/2s^{1.53}2p_z^{0.45}2p_x^{0.51}2p_y^{0.51}$$

We draw the following vbL diagram:

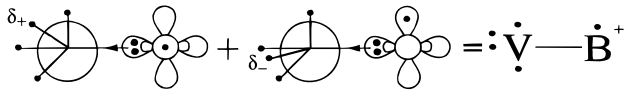

Electrons $3d_\pi$, $\delta_\pm$ on the metal, and $2p(\pi)$ on the B atom do not participate in the bonding process. Transfer of electrons through the π system and therefore bond formation is shut off due to the Pauli principle; this is clear from the superposition of the above diagrams, a half π bond in the one is canceled by the other. As far as the σ system is concerned, 3 e^- are distributed in the two hybrids: a $(4s4p_z3d_{z^2})^{1.0}$ on the V^+, and a $(2s2p_z)^{2.0}$ on the B atom. It seems that the two atoms are held together by a σ bond, but with no net electron transfer.

$19^6\Sigma^+$ State (5th of the Sextets). This is not an easily interpretable state in conventional terms. Three configurations are at least necessary for its description, namely,

$$\begin{aligned}19|^6\Sigma^+\rangle \approx\ & 0.29|1\sigma^2 2\sigma^1 1\delta_+^1 1\pi_x^1 1\pi_y^1 1\delta_-^1\rangle - \\ & 0.68|1\sigma^2 1\delta_+^1 3\sigma^1 1\pi_x^1 1\pi_y^1 1\delta_-^1\rangle + \\ & 0.39|1\sigma^2 2\sigma^1 1\delta_+^1 (1\pi_x^1 2\pi_y^1 + 2\pi_x^1 1\pi_y^1) 1\delta_-^1\rangle,\end{aligned}$$

the first two of which correspond to the $M = 0$ component ($X^6\Sigma^+$), with the third to the $M = \pm 1$, parental component, i.e., $|^5\mathrm{D};\ M = \pm 1\rangle \otimes |^2\mathrm{P};\ M = \mp 1\rangle$. The CAS equilibrium atomic distributions are

$$4s^{0.30}4p_z^{0.06}3d_{z^2}^{0.68}3d_{xz}^{0.58}3d_{yz}^{0.58}3d_{x^2-y^2}^{1.0}3d_{xy}^{1.0}/2s^{1.72}2p_z^{0.23}2p_x^{0.42}2p_y^{0.42}$$

very similar to those of the ground $X^6\Sigma^+$ state and of course of similar binding. The small binding energy, $D_e = 14.6$ kcal/mol at the MRCI level (Table 2), is due to the rather large coefficient (0.68) of the second configuration.

$22^6\Pi$ State (6th of the Sextets). The asymptotic description is given by the wave function $22|^6\Pi\rangle = |^5\mathrm{D};\ M = \pm 2\rangle \otimes |^2\mathrm{P};\ M = \mp 1\rangle$. As the interatomic distance decreases, and around 8 bohr, this state starts interacting strongly with the next, $28^6\Pi$ $|M = 0\rangle \otimes |M = \pm 1\rangle$ state, while close to equilibrium the interaction is diminished. Besides the numerical information given in Table 2 and the PEC in Figure 3, the bonding scheme is not clear.

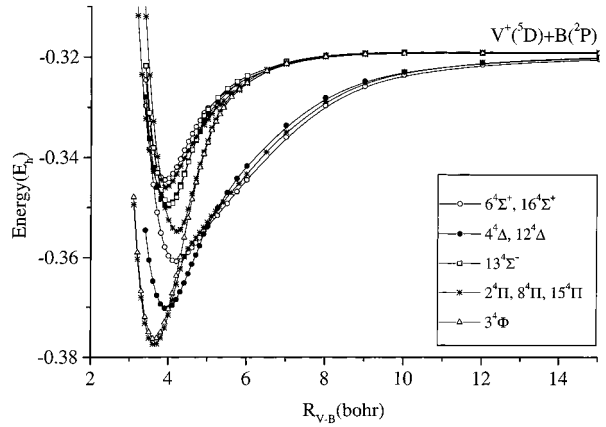

Figure 4. Potential energy curves of nine quartet states of Σ^+ (○), Σ^- (□), Π (∗), Δ (●), and Φ (△) spatial symmetry.

$27^6\Delta$, $28^6\Pi$, and $29^6\Sigma^-$ States (7th, 8th, and 9th of the Sextets). The above states are slightly bound with respect to the ground-state atoms, with D_e's 4.0, 3.8, and 3.2 kcal/mol, respectively; see Table 2. Figure 3 shows the corresponding PECs correlating to

$$27|^6\Delta\rangle = |^5\mathrm{D};\, M=\pm1\rangle \otimes |^2\mathrm{P};\, M=\pm1\rangle$$

$$28|^6\Pi\rangle = |^5\mathrm{D};\, M=0\rangle \otimes |^2\mathrm{P};\, M=\pm1\rangle$$

$$29|^6\Sigma^-\rangle = |^5\mathrm{D};\, M=\pm1\rangle \otimes |^2\mathrm{P};\, M=\mp1\rangle$$

4.2 Quartets. Table 3 and Figure 4 present numerical results and corresponding PECs of nine quartet states.

$2^4\Pi$ State (1st of the Quartets). At infinity, we have

$$2|^4\Pi\rangle = |^5\mathrm{D};\, M=\pm1\rangle \otimes |^2\mathrm{P};\, M=0\rangle$$

with the distribution $\sim 2s^2 3d^1_{x^2-y^2} 3d^1_{z^2} 2\bar{p}^1_z 3d^1_{xz} 3d^1_{xy}$. As we approach the equilibrium and around 4.4 bohr, an avoided crossing occurs between this and the 8th $^4\Pi$ ($|M=\pm2\rangle \otimes |M=\mp1\rangle$) state. This is clear from the PEC's morphology, the equilibrium CAS atomic distributions,

$$4s^{0.20}4p_z^{0.12}3d_{z^2}^{0.78}3d_{xz}^{1.0}3d_{yz}^{1.0}3d_{x^2-y^2}^{0.50}3d_{xy}^{0.50}/2s^{1.55}2p_z^{0.34}2p_x^{0.48}2p_y^{0.48}$$

and the leading configurations

$$2|^4\Pi\rangle \approx 0.61(|1\sigma^2 2\sigma^1 1\pi_x^2 1\pi_y^1 1\delta_-^1\rangle - |1\sigma^2 2\sigma^1 1\delta_+^1 1\pi_x^1 1\pi_y^2\rangle)$$

The above description is captured by the following vbL icon:

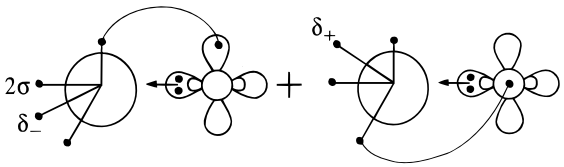

The superposition of the two pictures helps in explaining the nondelocalization of the single π (V^+) electron to a p_π B orbital. Therefore, the bonding is caused by a single π bond and a small electron transfer from B to V^+.

$3^4\Phi$ State (2nd of the Quartets). The energy difference between this and the previous state is 0.9 mhartree at the MRCI level; see Table 3. In fact, these two states are very similar, the difference being a "+" instead of a "−" sign in the leading configurations given above for the $2^4\Pi$ state. The same vbL diagram as before describes the bonding with a D_e and R_e practically equal to those of the $2^4\Pi$ state.

$4^4\Delta$ State (3rd of the Quartets). The history of this state is traced to the product $4|^4\Delta\rangle = |^5\mathrm{D};\, M=\pm2\rangle \otimes |^2\mathrm{P};\, M=0\rangle$. At equilibrium the leading configurations are

$$4|^4\Delta\rangle \approx 0.75|1\sigma^2 2\sigma^2 1\pi_x^1 1\pi_y^1 1\delta_-^1\rangle - 0.32|1\sigma^2 3\sigma^2 1\pi_x^1 1\pi_y^1 1\delta_-^1\rangle$$

with the following CAS equilibrium distributions

$$4s^{0.27}4p_z^{0.13}3d_{z^2}^{1.11}3d_{xz}^{0.78}3d_{yz}^{0.78}3d_{xy}^{1.0}/2s^{1.58}2p_z^{0.81}2p_x^{0.23}2p_y^{0.23}$$

The "0.32" configuration expresses the GVB correlation of the 2σ distribution. Through the σ frame 0.6 e^- are transferred from the sp_z hybrid of the B atom to the metal, with a synchronous back-donation via the π frame of 0.46 e^- from the metal to the B atom. Therefore, the emerging vbL icon is

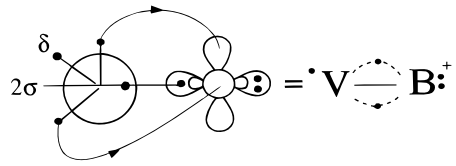

implying a σ bond and two half π bonds with a net transfer of 0.1 e^- from B to V^+, and an observer $\delta_-(3d_{xy})$ electron.

$6^4\Sigma^+$ State (4th of the Quartets). At infinity, we have $6|^4\Sigma^+\rangle = |^5\mathrm{D};\, M=0\rangle \otimes |^2\mathrm{P};\, M=0\rangle$, with the following leading equilibrium configurations and CAS populations,

$$6|^4\Sigma^+\rangle \approx 1\sigma^2 2\sigma^1 1\delta_+^1 1\pi_x^1 1\pi_y^1 1\delta_-^1\,(0.68\alpha\beta\beta\alpha\alpha\alpha\alpha - 0.21\alpha\beta\alpha\alpha\alpha\alpha\beta + 0.21\alpha\beta\alpha\beta\alpha\alpha\alpha) + 0.42|1\sigma^2 1\delta_+^1 3\bar{\sigma}^1 1\pi_x^1 1\pi_y^1 1\delta_-^1\rangle$$

$$4s^{0.19}4p_z^{0.09}3d_{z^2}^{0.21}3d_{xz}^{0.84}3d_{yz}^{0.84}3d_{x^2-y^2}^{1.0}3d_{xy}^{1.0}/2s^{1.62}2p_z^{0.85}2p_x^{0.18}2p_y^{0.18}$$

The vbL icon consistent with the above allocation is

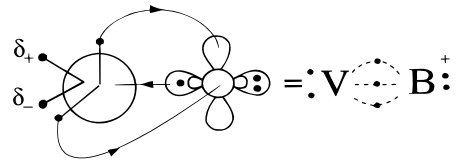

implying two half π bonds and a half σ bond. Obviously, 0.32 e^- diffuse from V^+ to B through the π system and 0.5 e^- from B to V^+ through the σ system, amounting to a total transfer from B to V^+ of 0.2 e^-. This state with a $D_e = 25.8$ kcal/mol at $R_e = 2.215$ Å (Table 3) and three half bonds, is similar to the $7^3\Delta_g$ and $1^2\Delta_g$ states of TiB^+ [1b] and ScB^+,[1a] respectively.

$8^4\Pi$ State (5th of the Quartets). Asymptotically, the description of the present state is given by $8|^4\Pi\rangle = |^5\mathrm{D};\, M=\pm2\rangle \otimes |^2\mathrm{P};\, M=\mp1\rangle$. As we approach the equilibrium, a first avoided crossing around 4.4 bohr occurs (see the $2^4\Pi$ state), while a second avoided crossing is encountered at about 3.9 bohr, and at the repulsive part of the PEC (Figure 4) with the 15th $^4\Pi$ state (vide infra). Our leading CASSCF configurations are

$$8|^4\Pi\rangle \approx 0.71|1\sigma^2 2\sigma^2 1\delta_+^1 1\pi_y^1 1\delta_-^1\rangle - 0.32|1\sigma^2 1\delta_+^1 3\sigma^2 1\pi_y^1 1\delta_-^1\rangle - 0.17(|1\sigma^2 2\sigma^1 1\pi_x^2 1\pi_y^1 1\delta_-^1\rangle - |1\sigma^2 2\sigma^1 1\delta_+^1 1\pi_x^1 1\pi_y^2\rangle)$$

The "0.71" component mirrors the asymptotic character of the

$2^4\Pi$ state, the "0.32" reflects its (left−right) GVB correlation, while the "0.17" component carries the memory of the $8^4\Pi$ adiabatic asymptote. The equilibrium CAS atomic populations

$$4s^{0.18}4p_z^{0.11}3d_{z^2}^{0.99}3d_{xz}^{0.14}3d_{yz}^{0.81}3d_{x^2-y^2}^{0.94}3d_{xy}^{0.94}/2s^{1.68}2p_z^{0.80}2p_x^{0.11}2p_y^{0.26}$$

are not very enlightening, other than the nonparticipation of the $\delta_\pm$ distributions in the bonding process. No vbL diagram can be drawn due to the entanglement of a significant number of configurations with relatively large coefficients.

$12^4\Delta$, $13^4\Sigma^-$, and $16^4\Sigma^+$ States (6th, 7th, and 9th of the Quartets). Asymptotically, all states above have the same spatial distribution; therefore, we can write, in an obvious notation,

$$|12^4\Delta,13^4\Sigma^-,16^4\Sigma^+\rangle = |^5\mathrm{D};\, M=\pm1,\mp1,\pm1\rangle \otimes |^2\mathrm{P};\, M=\pm1,\pm1,\mp1\rangle$$

Under C_{2v} symmetry restrictions, the $12^4\Delta$ state has two degenerate components of A_1 and A_2 spatial symmetry, with the following leading CAS configurations at infinity

$$12|^4\Delta\rangle = \begin{cases} |^4\mathrm{A}_1\rangle \approx 0.62|2s^2 3d_z{}^2 3d_{x^2-y^2}(3d_{xz}2\bar{p}_y - 2\bar{p}_x 3d_{yz})3d_{xy}\rangle \\ |^4\mathrm{A}_2\rangle \approx 0.62|2s^2 3d_z{}^2 3d_{x^2-y^2}(3d_{xz}2\bar{p}_x - 3d_{yz}2\bar{p}_y)3d_{xy}\rangle \end{cases}$$

The $13^4\Sigma^-$ and $16^4\Sigma^+$ states have an identical description with the $|^4A_2\rangle$ and $|^4A_1\rangle$ components, respectively, but with a "+" instead of a "−" sign. This similarity is reflected in the total energies and spectroscopic constants (Table 3) which are very similar for all three states. At equilibrium, the CAS leading configurations for the A_1 and A_2 components of the $12^4\Delta$ state are

$$|^4\mathrm{A}_1\rangle \approx 0.55|1\sigma^2 2\sigma^1 1\delta_+^1(1\pi_x^1 1\bar{\pi}_y^1 - 1\bar{\pi}_x^1 1\pi_y^1)1\delta_-^1) + 0.16|1\sigma^2 2\sigma^1 1\delta_+^1(1\pi_x^1 2\bar{\pi}_y^1 - 2\bar{\pi}_x^1 1\pi_y^1)1\delta_-^1\rangle - 0.15|1\sigma^2 2\sigma^1 1\delta_+^1(2\pi_x^1 2\bar{\pi}_y^1 - 2\bar{\pi}_x^1 2\pi_y^1)1\delta_-^1\rangle$$

$$|^4\mathrm{A}_2\rangle \approx 0.55|1\sigma^2 2\sigma^1 1\delta_+^1(1\pi_x^2 - 1\pi_y^2)1\delta_-^1\rangle - 0.16|1\sigma^2 2\sigma^1 1\delta_+^1(1\pi_x^1 2\bar{\pi}_x^1 - 1\pi_y^1 2\bar{\pi}_y^1)1\delta_-^1\rangle$$

The corresponding CAS populations of the $^4A_1$, practically identical with those of the $^4A_2$, are

$$4s^{0.20}4p_z^{0.10}3d_{z^2}^{0.73}3d_{xz}^{0.60}3d_{yz}^{0.60}3d_{x^2-y^2}^{0.95}3d_{xy}^{0.89}/2s^{1.60}2p_z^{0.54}2p_x^{0.40}2p_y^{0.40}$$

suggesting the following vbL descriptions in conjunction with the atomic asymptotic distributions

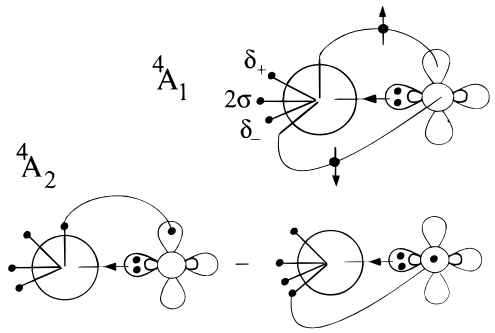

Notice the seemingly different binding descriptions of A_1 and A_2 symmetries; however, both are needed to describe correctly the $|\Lambda| = 2(\Delta)$ symmetry. Hence, we can say that the two atoms

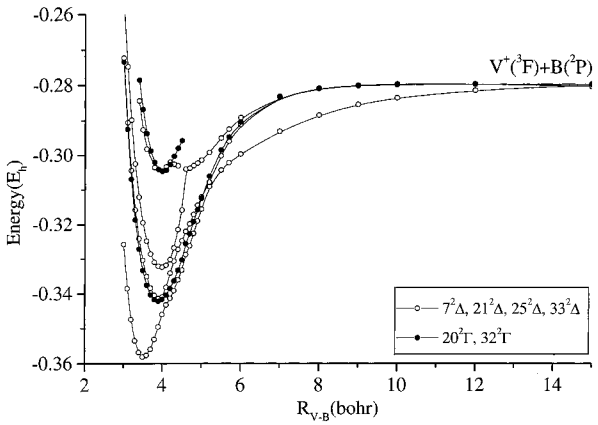

Figure 5. Potential energy curves of six doublet states of Δ (○) and Γ (●) spatial symmetry.

are held together by two half π bonds with their electrons coupled into a singlet, and a σ bond while ∼0.1 e^- is transferred from B to V^+.

The above discussion holds true in every detail for the $13^4\Sigma^-$ and $16^4\Sigma^+$ states, the only difference being a "+" sign instead of a "−" in the "0.55" component of the $^4A_2$ ($13^4\Sigma^-$) and the $^4A_1$ ($16^4\Sigma^+$) descriptions.

$15^4\Pi$ State (8th of the Quartets). As was already discussed, the $15^4\Pi$ state interacts strongly with the $8^4\Pi$ state around equilibrium, 3.9 bohr. The leading CASSCF equilibrium configurations are

$$15|^4\Pi\rangle \approx 0.75|1\sigma^2 1\delta_+^1 1\pi_x^2 1\pi_y^1 1\delta_-^1\rangle - 0.22|1\sigma^2 1\delta_+^1 2\pi_x^2 1\pi_y^1 1\delta_-^1\rangle + 0.30|1\sigma^2 1\delta_+^1 1\pi_x^1 2\bar{\pi}_x^1 1\pi_y^1 1\delta_-^1\rangle + 0.15|1\sigma^2 2\sigma^2 1\delta_+^1 1\pi_y^1 1\delta_-^1\rangle$$

The "0.75" component reflects the asymptotic behavior of the fragments, i.e., $|^5\mathrm{D};\, M=0\rangle \otimes |^2\mathrm{P};\, M=\pm1\rangle$, the "0.22" the GVB contribution, while the "0.15" component corresponds to the equilibrium configuration of the $8^4\Pi$ and to the asymptotic character of the $2^4\Pi$. The equilibrium CASSCF atomic populations

$$4s^{0.16}4p_z^{0.09}3d_{z^2}^{0.20}3d_{xz}^{1.01}3d_{yz}^{0.76}3d_{x^2-y^2}^{0.95}3d_{xy}^{0.95}/2s^{1.59}2p_z^{0.17}2p_x^{0.78}2p_y^{0.29}$$

in conjunction with the "0.75" component (of B_1 symmetry), dictates the following vbL picture

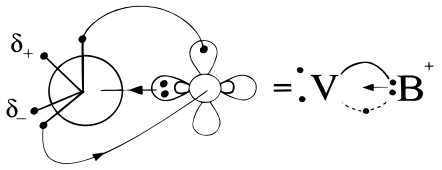

The bonding is essentially comprised of $1^1/_2$ π bonds, a σ bond while the $\delta_\pm$ electrons are practically localized on the metal; also, 0.15 e^- are transferred from B to V^+.

4.3. Doublets. Table 4 and Figures 5−7 condense numerical results and corresponding PECs of 16 doublets, 12 of which correlate to the second excited $^3F(4s^13d^3)$ state of V^+.

$7^2\Delta$, $21^2\Delta$, $25^2\Delta$, and $33^2\Delta$ States (1st, 8th, 11th, and 16th of the Doublets). Asymptotically, we can write

$$|7^2\Delta,21^2\Delta,25^2\Delta\rangle = |^3\mathrm{F};\, \mathrm{M}=\pm2,\pm3,\pm1\rangle \otimes |^2\mathrm{P};\, M=0,\mp1,\pm1\rangle$$

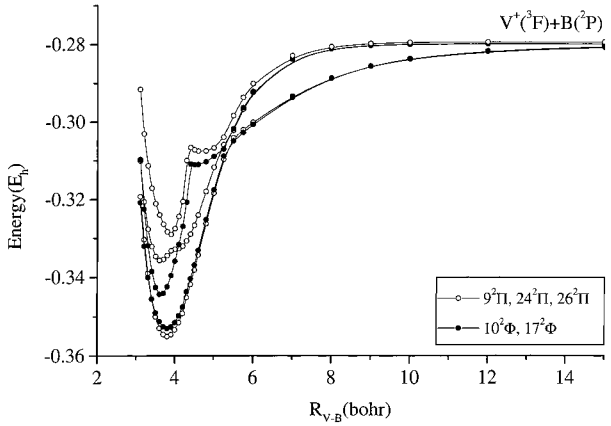

Figure 6. Potential energy curves of five doublet states of Π (○) and Φ (●) spatial symmetry.

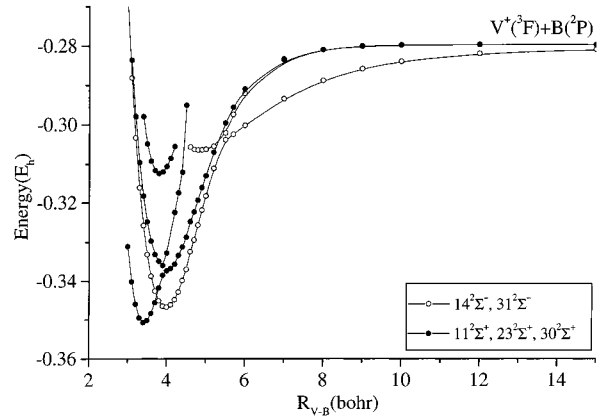

Figure 7. Potential energy curves of five doublet states of Σ^- (○) and Σ^+ (●) spatial symmetry.

and $33|^2\Delta\rangle = |^3\mathrm{P}(3d^4);\ M = \pm1\rangle \otimes |^2\mathrm{P};\ M = \pm1\rangle$. The main CAS equilibrium configurations and populations of the $7^2\Delta$ state are

$$\approx 0.86|1\sigma^2 1\delta_+^1 1\pi_x^2 1\pi_y^2\rangle - 0.19|1\sigma^2 1\delta_+^1(1\pi_x^2 2\pi_y^2 + 2\pi_x^2 1\pi_y^2)\rangle$$

$$4s^{0.18}4p_z^{0.09}3d_{z^2}^{0.23}3d_{xz}^{1.27}3d_{yz}^{1.27}3d_{x^2-y^2}^{1.0}/2s^{1.46}2p_z^{0.08}2p_x^{0.65}2p_y^{0.65}$$

giving rise to the following vbL icon:

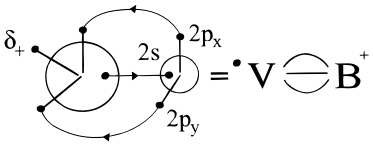

It is worthwhile to discuss the bonding process as we move from infinity toward equilibrium. Till about 5.5 bohr, the infinity character is maintained; at this point, an avoided crossing occurs with the $21^2\Delta$ state. Moving further to the left, a second avoided crossing takes place at about 4 bohr with the $21^2\Delta$ state again, which has already suffered a second avoided crossing around 4.2 bohr with the $25^2\Delta$ state (Figure 5). However, the equilibrium character of the $7^2\Delta$ state mirrors that of the $33^2\Delta$ state due to an avoided crossing of the latter with the $25^2\Delta$ state at about 4.5 bohr. Notice further that the $33^2\Delta$ *diabatically* correlates to the first excited state of the B atom (^{4}P; $2s^12p^2$), 3.57 eV above the ground ^{2}P state (Table 1). That the in situ B atom finds itself in the ^{4}P state is evidenced from the equilibrium population distributions. The vbL picture captures the physics of the bonding, clearly indicating the formation of three bonds, two π and one σ; about 0.6 e^- are transferred from B to V^+ via the π frame, and 0.5 e^- from V^+ to B through the σ skeleton. The binding energy with respect to the adiabatic products is 49.2 kcal/mol at $R_e = 1.858$ Å; see Table 4. With the exception of the $11^2\Sigma^+$ state which also forms a triple bond, the $7^2\Delta$ state has the shortest bond length of all other states. However, with respect to the ground-state atoms, the $D_e = 49.2 - \Delta E(^3\mathrm{F} \leftarrow {}^5\mathrm{D}) = 24.7$ kcal/mol, but with an "internal bond strength" (with respect to $V^+(^5\mathrm{D}) + \mathrm{B}(^4\mathrm{P})) = 107$ kcal/mol. This last value compares favorably with the isovalent triple bonded species, $V{-}CH^+$ ($X^2\Delta$) with $D_e = 108$ kcal/mol at $R_e = 1.745$ Å.[16]

The $21^2\Delta$ state suffers three avoided crossings, two of which at 5.5 and 4.0 bohr have already been discussed (vide supra). These two sequential avoided crossings reestablish the initial (asymptotic) character of the state, as is evidenced from the leading configurations of the repulsive part of the PEC (Figure 5). The third avoided crossing occurs around 4.2 bohr, introducing ~20% triple bond character in the bonding evolution process. At equilibrium ($R_e = 2.053$ Å, $D_e = 39.2$ kcal/mol; Table 4) the bonding cannot be described by simple vbL icons due to its intense multiconfiguration character.

The $25^2\Delta$ state's PEC presents two avoided crossings, the first at about 4.6 bohr with the $33^2\Delta$ state and a second avoided crossing around 4.2 bohr with the $21^2\Delta$ state. The leading CAS equilibrium configurations are

$$25|^2\Delta\rangle \approx 0.16|1\sigma^2 1\delta_+^1 1\pi_x^2 1\pi y^2\rangle - 0.45|1\sigma^2 2\sigma^2 1\pi_x^1 1\pi_y^1 1\bar{\delta}_-^1\rangle + 0.22|1\sigma^2 2\sigma^2(1\pi_x^1 1\bar{\pi}_y^1 + 1\bar{\pi}_x^1 1\pi_y^1)1\delta_-^1\rangle$$

The "0.16" component mirrors the triple bond character due to the excited ^{4}P state of boron, with the (−0.45, 0.22) vector reflecting the asymptotic character of the $7^2\Delta$ state. No simple bonding picture of this state can be given.

A part, around equilibrium, of the $33^2\Delta$ PEC is shown in Figure 5; we were unable to compute the full PEC for technical reasons. This state must correlate to the $^3\mathrm{P}(3d^4)$ state of the metal. The only information that can be given for the $33^2\Delta$ state is an approximate $R_e \approx 4$ bohr.

$9^2\Pi$, $24^2\Pi$, and $26^2\Pi$ States (2nd, 10th, and 12th of the Doublets). The asymptotic (atomic) behavior can be represented by the wave function

$$|9^2\Pi,24^2\Pi,26^2\Pi\rangle = |^3\mathrm{F};\ M = \pm1,\pm2,0\rangle \otimes |^2\mathrm{P};\ M = 0,\mp1,\pm1\rangle$$

Moving from infinity toward equilibrium, the $9^2\Pi$ state interacts strongly with the $24^2\Pi$ giving rise to an avoided crossing at around 5.5 bohr; see Figure 6. It would be expected that the character of the $9^2\Pi$ state would be conveyed to the $24^2\Pi$ state; however, the $26^2\Pi$ state intervenes lending its character to the $24^2\Pi$, while the former aquires the features of the $9^2\Pi$. Overall, the 9th correlates to the asymptotic products of the 24th, the 24th to the asymptotic products of the 26th, and the 26th to the products of the 9th. The CAS equilibrium leading configurations and populations of the $9^2\Pi$ state are

$$9|^2\Pi\rangle \approx 0.46(|1\sigma^2 2\bar{\sigma}^1 1\delta_+^1 1\pi_x^1 1\pi_y^2\rangle - |1\sigma^2 2\bar{\sigma}^1 1\pi_x^2 1\pi_y^1 1\delta_-^1\rangle)$$

$$4s^{0.30}4p_z^{0.12}3d_{z^2}^{0.47}3d_{xz}^{1.07}3d_{yz}^{1.07}3d_{x^2-y^2}^{0.50}3d_{xy}^{0.50}/2s^{1.43}2p_z^{0.69}2p_x^{0.39}2p_y^{0.39}$$

The above populations evolve naturally from the asymptote of

the $24^2\Pi$ state. The vbL diagram

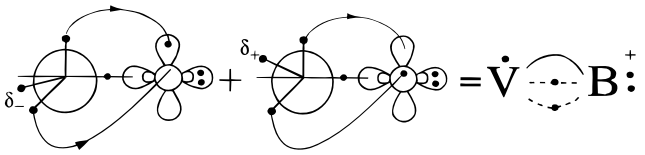

suggests a π bond, a half π bond and a half σ bond. Along the σ skeleton, two strong hybrids dominate, a $(4s4p_z3d_{z^2})^{0.90}$ on the V^+ and a $(2s2p_z)^{2.1}$ on the B atom. Via the σ frame, $\sim$0.1 e^- are transferred from V^+ to B, while through the π frame, $\sim$0.2 e^- are transferred from B to V^+.

The $24^2\Pi$ state suffers an avoided crossing with the $9^2\Pi$ state around 5.5 bohr (vide supra), with a second and a third avoided crossing occurring at 5.25 and 3.9 bohr, respectively, with the $26^2\Pi$ state (Figure 6). As a result of the "5.25" avoided crossing, a shallow minimum is observed just before the third avoided crossing. At equilibrium, the leading CAS configurations are

$$24|^2\Pi\rangle \approx -0.50|1\sigma^2 2\sigma^2 1\pi_x^1 1\pi_y^2\rangle + 0.28(|1\sigma^2 2\sigma^1 1\bar{\delta}_+^1 1\pi_x^1 1\pi_y^2\rangle - |1\sigma^2 2\sigma^1 1\pi_x^2 1\pi_y^1 1\bar{\delta}_-^1\rangle) - 0.32(|1\sigma^2 2\sigma^1 1\delta_+^1 1\bar{\pi}_x^1 1\pi_y^2\rangle - |1\sigma^2 2\sigma^1 1\pi_x^2 1\bar{\pi}_y^1 1\delta_-^1\rangle)$$

The "-0.50" component mirrors the $26^2\Pi$ asymptote, while the "0.28, -0.32" components seems to correlate *diabatically* to $V^+(^3P;\ 3d^4) + B(^2P)$ products (Figure 6). The CAS atomic populations are not very informative; however, the above given configurations support the following "resonance" valence bond structures

The $26^2\Pi$ suffers three avoided crossings, one at 5.25 bohr with the $24^2\Pi$ state, a second at 4.4 bohr, and a third one around 4.0 bohr with the $24^2\Pi$ state again. As a result, the corresponding PEC presents a local minimum around 4.6 bohr reflecting the $9^2\Pi$ asymptote (Figure 6). This is also corroborated from the CAS equilibrium atomic populations which are practically the same with the asymptotic populations of the $9^2\Pi$ state. The bonding is mainly due to a σ interaction between an sp_z hybrid on the B atom and a $3d_{z^2}$ orbital of the V^+ cation. A total of 0.3 e^- are transferred from B to V^+ via the σ frame. As expected at the global minimum ($\sim$3.9 bohr), the bonding is comprised by the above given resonance valence bond structures. The binding energies and interatomic distances of the $9^2\Pi$, $24^2\Pi$, and $26^2\Pi$ state are 47.2, 35.0, 31.1 kcal/mol at 2.009, 1.921, and 2.055 Å, respectively, with respect to the adiabatic products (Table 4).

$10^2\Phi$ and $17^2\Phi$ States (3rd, and 6th of the Doublets). The asymptotes of the above states are described by

$$|10^2\Phi, 17^2\Phi\rangle = |^3F;\ M = \pm3, \pm2\rangle \otimes |^2P;\ M = 0, \pm1\rangle$$

or in terms of real atomic orbitals

$$10|^2\Phi\rangle \approx 0.49(|2s^2 4\bar{s}^1 3d_{z^2}^1 2\bar{p}_z^1 3d_{yz}^1 3d_{xy}^1\rangle + |2s^2 4\bar{s}^1 3d_{x^2-y^2}^1 3d_{z^2}^1 2\bar{p}_z^1 3d_{xz}^1\rangle)$$

$$17|^2\Phi\rangle \approx 0.49(|2s^2 4\bar{s}^1 3d_{x^2-y^2}^1 3d_{xz}^1 3d_{yz}^1 2\bar{p}_y^1\rangle + |2s^2 4\bar{s}^1 3d_{xz}^1 2\bar{p}_x^1 3d_{yz}^1 3d_{xy}^1\rangle)$$

The two states interchange their M values after an avoided crossing at 5.25 bohr (Figure 6); subsequently, the $17^2\Phi$ state suffers a second avoided crossing at about 4.3 bohr, possibly with a state originating from a $^3H(V^+)$ state.

The main spin coupled CAS equilibrium configurations are as follows

$$10|^2\Phi\rangle \approx 0.47(|1\sigma^2 2\bar{\sigma}^1 1\delta_+^1 1\pi_x^1 1\pi_y^2\rangle + |1\sigma^2 2\bar{\sigma}^1 1\pi_x^2 1\pi_y^1 1\delta_-^1\rangle)$$

$$17|^2\Phi\rangle \approx 0.48(|1\sigma^2 2\sigma^1 1\bar{\delta}_+^1 1\pi_x^1 1\pi_y^2\rangle + |1\sigma^2 2\sigma^1 1\pi_x^2 1\pi_y^1 1\bar{\delta}_-^1\rangle)$$

The similarity of the equilibrium and the asymptotic character between the $10^2\Phi$ and the $17^2\Phi$ states, respectively, is obvious. The equilibrium configurations of the $17^2\Phi$ state reflect the configurations of the second avoided crossing. The equilibrium distributions are

$$10|^2\Phi\rangle:\ 4s^{0.29}4p_z^{0.12}3d_{z^2}^{0.45}3d_{xz}^{1.10}3d_{yz}^{1.10}3d_{x^2-y^2}^{0.50}3d_{xy}^{0.50}/2s^{1.43}2p_z^{0.69}2p_x^{0.38}2p8_y^{0.38}$$

$$17|^2\Phi\rangle:\ 4s^{0.24}4p_z^{0.11}3d_{z^2}^{0.73}3d_{xz}^{0.98}3d_{yz}^{0.98}3d_{x^2-y^2}^{0.50}3d_{xy}^{0.50}/2s^{1.44}2p_z^{0.48}2p_x^{0.48}2p_y^{0.48}$$

leading to the following vbL icon for both states

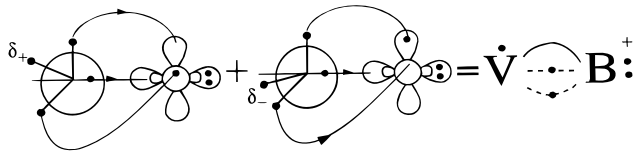

We have clearly a π bond, a half π bond, a half σ bond, and a $\delta_\pm$ observer electron. For reasons of completeness, it is reminded that the above description pertains to the B_1 component of the Φ symmetry.

$11^2\Sigma^+$, $23^2\Sigma^+$, and $30^2\Sigma^+$ States (4th, 9th, and 13th of the Doublets). The above doublets trace their lineage to

$$11|^2\Sigma^+\rangle = |^3F;\ M = \pm1\rangle \otimes |^2P;\ M = \mp1\rangle$$

$$23|^2\Sigma^+\rangle = |^3P(3d^4);\ M = \pm1\rangle \otimes |^2P;\ M = \mp1\rangle$$

$$30|^2\Sigma^+\rangle = |^3H(3d^4);\ M = ?\rangle \otimes |^2P;\ M = ?\rangle$$

The asymptotic behavior of the $11^2\Sigma^+$ state is captured by the CAS leading configurations

$$11|^2\Sigma^+\rangle \approx 0.31|2s^2 4\bar{s}^1 3d_{x^2-y^2}^1(3d_{xz}^1 2\bar{p}_y^1 + 2\bar{p}_x^1 3d_{yz}^1)3d_{xy}^1\rangle + 0.27|2s^2 4\bar{s}^1 3d_{z^2}^1 3d_{x^2-y^2}^1(3d_{xz}^1 2\bar{p}_x^1 - 3d_{yz}^1 2\bar{p}_y^1)\rangle + 0.27|2s^2 4\bar{s}^1 3d_{z^2}^1(3d_{xz}^1 2\bar{p}_y^1 - 2\bar{p}_x^1 2d_{yz}^1)3d_{xy}^1\rangle$$

Moving toward equilibrium, the character of these configurations is retained till 3.9 bohr; at this point, a severe avoided crossing occurs with the $23^2\Sigma^+$ state, which had already suffered an avoided crossing around 4.5 bohr with an incoming state tracing its ancestry to an excited $^4P(2s^12p^2)$ state of the B atom (Figure 7). This last avoided crossing is responsible for conveying the triple bonded character to the VB^+ species in the $11^2\Sigma^+$ state (vide infra).

The most relevant CAS equilibrium configuration and populations are

$$11|^2\Sigma^+\rangle \approx 0.82|1\sigma^2 2\sigma^1 1\pi_x^2 1\pi_y^2\rangle$$

$$4s^{0.25}4p_z^{0.12}3d_{z^2}^{0.84}3d_{xz}^{1.28}3d_{yz}^{1.28}3d_{x^2-y^2}^{0.13}3d_{xy}^{0.13}/2s^{1.47}2p_z^{0.33}2p_x^{0.53}2p_y^{0.53}$$

clearly suggesting the following picture

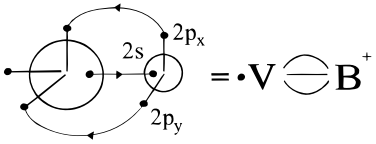

indicating a triple bonded VB^+ species. Along the π-system, about 0.9 e^- are migrating from B to V^+, and via the σ frame, 0.80 e^- are moving from V^+ to B. The triple bond is reflected in the bond distance which is the smallest of all states studied, 1.804 Å and $D_e = 44.6$ kcal/mol at the MRCI level with respect to the adiabatic products (Table 4) or 20.0 kcal/mol with respect to the ground-state products, $V^+(^5D) + B(^2P)$ (Table 1). However, the *internal bond strength*, i.e., with respect to the *diabatic products* $V^+(^5D) + B(^4P)$, is 102.3 kcal/mol, very similar to the $7^2\Delta$ state as it should (vide supra).

Nothing much can be said about the $23^2\Sigma^+$ state other than that, at a not well-defined equilibrium distance (2.06 Å), its character carries the memory of the excited ^4P state of B and of the $11^2\Sigma^+$ state. An approximate binding energy with respect to the adiabatic products can be given, by employing the experimental energy difference of $V^+(^3P \leftarrow {}^3F) = 8.0$ kcal/mol,[13] thus $D \approx 43$ kcal/mol.

For the $30^2\Sigma^+$, only a small part of the PEC around the equilibrium (2.016 Å, Table 4) has been constructed. The binding character is unclear due to a multitude of equally contributing configurations.

$14^2\Sigma^-$ and $31^2\Sigma^-$ States (5th and 14th of the Doubles). The asymptotic behavior is described by the product

$$|14^2\Sigma^-,31^2\Sigma^-\rangle = |^3F;\, M = 0, \pm 1\rangle \otimes |^2P;\, M = 0, \mp 1\rangle$$

An avoided crossing between these two states occurs around 5.2 bohr; see Figure 7. Due to the avoided crossing the bonding character of the $14^2\Sigma^-$ correlates to the asymptotic configurations of the $31^2\Sigma^-$ state and vice versa. What is clear concerning the $14^2\Sigma^-$ state from the equilibrium and the asymptotic configurations, in conjunction with the atomic CAS distributions,

$$4s^{0.46}4p_z^{0.13}3d_{z^2}^{0.89}3d_{xz}^{0.65}3d_{yz}^{0.65}3d_{x^2-y^2}^{0.70}3d_{xy}^{0.70}/2s^{1.46}2p_z^{0.78}2p_x^{0.34}2p_y^{0.34}$$

is the formation of a σ and a π bond.

In the $31^2\Sigma^-$ state, whose PEC is not complete due to technical reasons, the character of the asymptotic behavior of the $14^2\Sigma^-$ state is transferred to the equilibrium of the $31^2\Sigma^-$ as is evidenced from the (equilibrium) configurations and the atomic populations. As a result, only a σ bond is formed with the π and δ electrons being localized on the metal. Overall, 0.3 e^- are transferred through the σ frame from B to V^+.

The bonding mechanism of the 14th and $31^2\Sigma^-$ states is reflected in the bond distances and dissociation energies which are 2.104 and 2.549 Å and 41.5 and 16.8 kcal/mol, respectively, with respect to the adiabatic products. Notice that the $31^2\Sigma^-$ state is unbound with respect to the ground-state products.

$20^2\Gamma$ and $32^2\Gamma$ States (7th and 11th of the Doublets). The PECs of the above states are presented in Figure 5. Due to purely technical difficulties, the $32^2\Gamma$ PEC has been only partially constructed. It is assumed that this state correlates to the $^3H(3d^4)$ state of the V^+ atom. At the MRCI level of theory only, the bond distance is well defined, $R_e = 2.119$ Å; see Table 4.

The $20^2\Gamma$ state correlates to the product $|^3F;\, M = \pm 3\rangle \otimes |^2P;\, M = \pm 1\rangle$. The leading CAS equilibrium configurations are

$$20|^2\Gamma\rangle \approx 0.37\{|1\sigma^2 2\sigma^2 1\delta_+^1(1\pi_x^2 - 1\pi_y^2)\rangle - |1\sigma^2 2\sigma^2(1\pi_x^1 1\bar{\pi}_y^1 - 1\bar{\pi}_x^1 1\pi_y^1)1\delta_-^1\rangle\}$$

representing faithfully the asymptotic distributions. In conjunction with the atomic equilibrium populations

$$4s^{0.38}4p_z^{0.14}3d_{z^2}^{1.19}3d_{xz}^{0.66}3d_{yz}^{0.66}3d_{x^2-y^2}^{0.50}3d_{xy}^{0.50}/2s^{1.49}2p_z^{0.75}2p_x^{0.33}2p_y^{0.33}$$

and the populations at infinity, we can clearly suggest that the atoms are held together by a π and σ bond. A better understanding of the bond formation can be grasped by the vbL icons

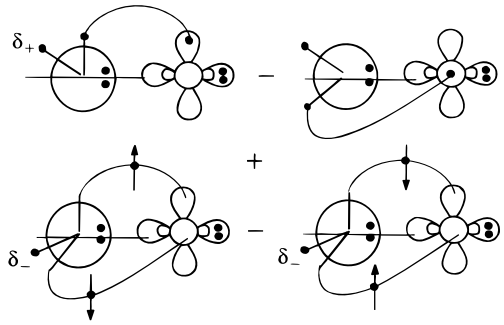

Notice the nonconventional π bond character; two strong hybrids, $(4s4p_z3d_{z^2})^{1.70}$ and $(2s2p_z)^{2.24}$ on the V^+ and B atoms, respectively, are responsible for the σ bond. The $1.70 + 2.24 = 4 - (0.03 + 0.03)_{GVB}$ e^-, where the 2×0.03 e^- corresponds to the GVB correlation on the $2p_x$ and $2p_y$ functions, from the σ skeleton.

5. Synopsis and Final Remarks

Employing MRCI techniques (CASSCF + 1 + 2) and quantitative bases, we have calculated the ground ($X^6\Sigma^+$) and 33 excited states ($\Sigma^\pm$, Π, Δ, Φ, and Γ symmetries) of the seven "valence" electron molecule VB^+. For most of the states, we report absolute energies, dissociation energies, bond lengths, harmonic frequencies, energy gaps, and full potential energy curves. Partial information is given for the $23^2\Sigma^+$, $30^2\Sigma^+$, $31^2\Sigma^-$, $32^2\Gamma$, and $33^2\Delta$ states, mainly due to technical difficulties. An assessment of the errors involved in our calculations is given in ref 1b; as in TiB^+,[1b] we estimate that our MRCI D_e values are underestimated by about 2.5 kcal/mol, or an average error of 5%. Our findings can be summarized as follows

(1) The 33 excited states studied span an energy range of about 2.5 eV; see Figure 2.

(2) All states are bound with respect to the adiabatic products, with binding energies ranging from $49.2(7^2\Delta)$ to $3.2(29^6\Sigma^-)$ kcal/mol. However, with respect to the ground-state products, four of them, namely, the $30^2\Sigma^+$, $31^2\Sigma^-$, $32^2\Gamma$, and $33^2\Delta$, are unbound.

(3) The $7^2\Delta$ and $11^2\Sigma^+$ states are clearly triple bonded with *internal bond strengths* of 107 and 102 kcal/mol, respectively.

(4) Obviously, for states very close in (absolute) energy (see Figure 2), we are not sure of their ordering.

(5) Through the states studied, a variety of bonding modes are observed, ranging from three full bonds ($2\pi + 1\sigma$) to a single bond (σ or π).

(6) It is interesting to observe that all the ground states of the species ScB^+,[1a] TiB^+,[1b] VB^+, and CrB^+ [17] have high-spin ground states, namely, $^4\Sigma^-$, $^5\Delta$, $^6\Sigma^+$, and $^7\Sigma^+$, respectively, with similar binding modes: three half bonds with zero, one (1δ), two (2δ), and three (2δ, 1σ) "observer", symmetry carrying electrons. This bonding similarity is reflected in the D_e and R_e values for the first three species: 44.9, 44.6, and 42.7, at 2.160, 2.102, and 2.061 Å, respectively. The CrB^+ with a $D_e = 27.0$ kcal/mol at $R_e = 2.335$ Å [17] deviates drastically from the previously given values. This deviation could be attributed to an extra 3σ electron on the Cr^+ cation interacting repulsively with the incoming σ electron on the B atom.

Acknowledgment. The financial support of the National and Kapodistrian University of Athens through its Special Research Account for Basic Research is greatly appreciated.

References and Notes

(1) (a) Kalemos, A.; Mavridis, A. *Adv. Quantum Chem*. **1998**, *32*, 69. (b) Kalemos, A.; Mavridis, A. *J. Phys. Chem. A* **1998**, *102*, 5982.
(2) Bauschlicher, C. W., Jr. *Theor. Chim. Acta* **1995**, *92*, 183.
(3) Dunning, T. H., Jr. *J. Chem. Phys.* **1989**, *90*, 1007.
(4) See, for instance: Couty, M.; Hall, M. B. *J. Phys. Chem. A* **1997**, *101*, 6936.
(5) Bartlett, R. J. *Annu. Rev. Phys. Chem.* **1981**, *32*, 359.
(6) Duch, W.; Diercksen, G. H. F. *J. Chem. Phys.* **1994**, *101*, 3018.
(7) Werner, H.-J.; Knowles, P. J. *J. Chem. Phys*. **1988**, *89*, 5803. Knowles, P. J.; Werner, H.-J. *Chem. Phys. Lett*. **1988**, *145*, 514. Werner, H.-J.; Reinsch, E. A. *J. Chem. Phys*. **1982**, *76*, 3144. Werner, H.-J. *Adv. Chem. Phys*. **1987**, *LXIX*, 1.
(8) Docken, K.; Hinze, J. *J. Chem. Phys*. **1972**, *57*, 4928.
(9) Werner, H.-J.; Meyer, W. *J. Chem. Phys.* **1981**, *74*, 5794.
(10) MOLPRO is a package of ab initio programs written by H.-J. Werner and P. J. Knowles, with contributions from J. Almlöf, R. D. Amos, A. Berning, M. J. O. Deegan, F. Eckert, S. T. Elbert, C. Hambel, R. Lindh, W. Meyer, A. Nicklass, K. Peterson, R. Pitzer, A. J. Stone, P. R. Taylor, M. E. Mura, P. Pulay, M. Schuetz, H. Stoll, T. Thorsteinsson, and D. L. Cooper.
(11) Partridge, H. *J. Chem. Phys*. **1989**, *90*, 1043.
(12) Koga, T.; Tatewaki, H.; Thakkar, A. *J. Chem. Phys*. **1994**, *100*, 8140.
(13) Moore, C. E. *Atomic energy Levels*; NSRDS−NBS Circular 3; U. S. GPO: Washington, DC, 1971.
(14) Roothaan, C. C. J. *Rev. Mod. Phys*. **1951**, *23*, 69.
(15) Bloomberg, M. R. A.; Sieghbahn, P. E. M. *J. Chem. Phys*. **1983**, *78*, 5682.
(16) Mavridis, A.; Alvarado-Swaisgood, A. E.; Harrison, J. F. *J. Phys. Chem*. **1986**, *90*, 2584.
(17) Kalemos, A.; Mavridis, A. Manuscript in preparation.